NUMERICAL INVESTIGATION OF TURBULENT NATURAL CONVECTION IN AN INCLINED SQUARE ENCLOSURE

Qasim S. Mehdi
College of Engineering
University of Mustansiriya

Khudheyer S. Mushatet
College of Engineering
University of Thiqar

ABSTRACT

Two dimensional turbulent natural convection heat transfer and fluid flow inside an air filled inclined square enclosure differentially heated has been numerically studied. Fully elliptic Navier- Stockes and energy equations are solved using finite volume method. The problem is simulated for different angles of inclination ($0 \le \theta \le 180 \deg.$) and Rayleigh numbers ($10^8 \le Ra \le 10^{16}$). The turbulence k-ϵ model is used to model the effect of turbulence. The wall function approach is used to model the regions near the walls of the enclosure. The obtained results from this study show that the rate of heat transfer is increased with the increase of Rayleigh number and decreased with the increase of angle of inclination($0 \le \theta \le 90 \deg.$).Also the induced vortices are strongly elongated with increase of Rayleigh number. The thickness of thermal boundary layer is decreased with the increase of Ra. The validation of the present code was done by comparing the computed results with the published ones. The comparison indicated a good agreement.

المستخلص: أجريت دراسة عددية لدراسة انتقال الحرارة وجريان المائع بالحمل الحر الأضطرابي داخل حيز مربع مائل ومسخن تسخينا جزئيا. تم حل معادلات نافير– ستوكس ومعادلة الطاقة باستخدام طريقة الحجم المحدد. أجريت الدراسة الحالية لزوايا ميلان مختلفه($0 \le \theta \le 180 \deg.$) ولأرقام رايلة متعددة($10^8 \le Ra \le 10^{16}$) بينما تم استخدام نموذج الأضطراب (k-ϵ) لمعالجة تأثير الأضطراب. أستخدم اسلوب دالة الجدار لنمذجة المناطق القريبة جدا من الجدران. أظهرت النتائج التي تم الحصول عليها أن معدل انتقال الحرارة قد ازداد مع زيادة عدد رايلة ويقل بزيادة زاوية الميلان($0 \le \theta \le 90$ deg). أيضا بينت النتائج أن الدوامات الناتجة تستطيل وتتحد بقوة مع زيادة عدد رايلة بينما يقل سمك الطبقة الحرارية المتاخمة. تم التأكد من صحة الطريقة العددية المستخدمة من خلال المقارنة مع النتائج العملية المنشورة حيث بينت المقارنة توافقا جيدا.

KEYWORDS

natural convection, heat transfer, enclosed enclosure

INTRODUCTION

Natural convection heat transfer in an enclosure is of importance in many engineering applications. These include cooling of electronic systems, double windows, air gaps in unventilated spaces and solar collectors.. However turbulent natural convection in inclined enclosures is still needs more research area to understand the complex fluid flow and heat transfer behavior. In the reviewed studies on natural convection, there is a few studies relating the turbulent natural convection inside inclined enclosures, so the present study try to facillate the challenge in understanding the flow and heat transfer behavior in this type of the problems. One of the most important bench mark studies on turbulent natural convection inside enclosed cavities was an experimental study done by(**Ampofo and Karayiannis,2003**). (**Corcione,2003**) performed a numerical study on the natural convection in a rectangular horizontal enclosure differentially heated. He used various thermal conditions of the cavity side walls. Also laminar natural convection in enclosed cavities has been studied numerically and experimentally by (**Davis to Kuper et al**., **1983-1993**). (**Markatos et al.,1984**) and **(Lankhorst et al., 1991)** used a k-ϵ model to study the two and three dimensional turbulent flows inside a cavity. Some interesting studies for both laminar and turbulent flows in inclined cavities has been found by the authors (**Zhongand Young,1985**) and(**Elshirbiny,1982**).

In the present work a numerical investigation has been performed to study the turbulent 2D thermally driven air flows inside a square enclosure. The objective was to investigate how the enclosure tilted angle can effect on these flows which are found in a diverse engineering applications. The computations were performed for Ra ranging from 10^8 to 10^{16} and an angle of inclination from 0° to 180°. The enclosure is differentially heated as shown in **Fig**.**1**.

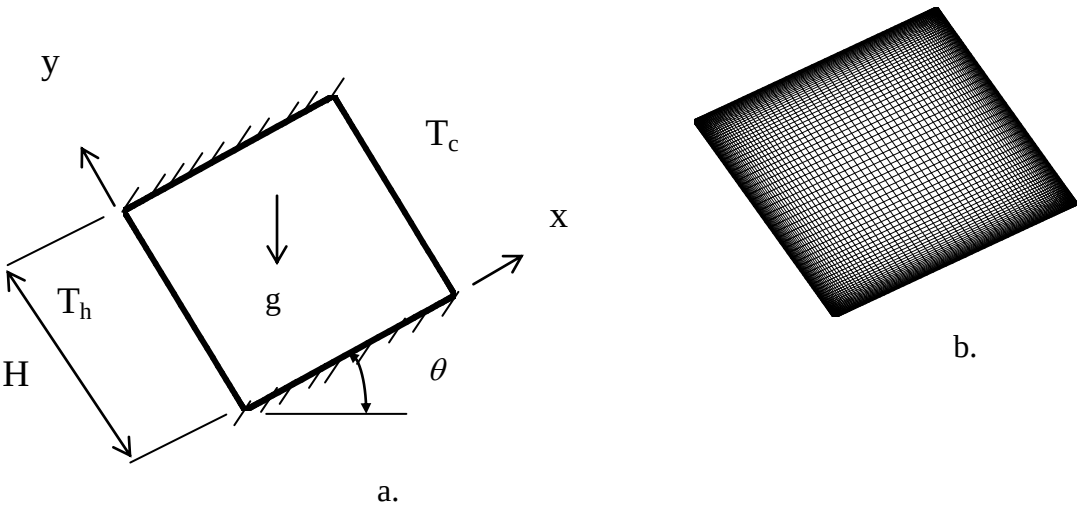

Fig.1. problem of interest; (a) physical domain , (b) computational domain

MATHEMATICAL MODEL

The turbulent viscous flow and temperature distribution inside an inclined square enclosure are described by the steady Navier-Stockes, energy and turbulence equations. The flow is assumed to be incompressible and Boussine approximation is valid. Employing the eddy viscosity concept, the time averaged governing equations are defined as follows(**Jones and Luander,1972)**:

$$\frac{\partial u}{\partial x}+\frac{\partial v}{\partial y}=0 \quad (1)$$

$$\rho u\frac{\partial u}{\partial x}+\rho v\frac{\partial u}{\partial y}=-\frac{\partial p}{\partial x}+2\frac{\partial}{\partial x}\left(\mu_{eff}\frac{\partial u}{\partial x}\right)+\frac{\partial}{\partial y}\left(\mu_{eff}\frac{\partial u}{\partial y}\right)+\frac{\partial}{\partial y}\left(\mu_{eff}\frac{\partial v}{\partial x}\right)+\rho g\beta(T-T_0)\sin\theta \quad (2)$$

$$\rho u\frac{\partial v}{\partial x}+\rho v\frac{\partial v}{\partial y}=-\frac{\partial p}{\partial y}+\frac{\partial}{\partial x}\left(\mu_{eff}\frac{\partial v}{\partial x}\right)+2\frac{\partial}{\partial y}\left(\mu_{eff}\frac{\partial v}{\partial y}\right)+\frac{\partial}{\partial x}\left(\mu_{eff}\frac{\partial u}{\partial y}\right)+\rho g\beta(T-T_0)\cos\theta \quad (3)$$

$$\rho u\frac{\partial T}{\partial x}+\rho v\frac{\partial T}{\partial y}=\frac{\partial}{\partial x}\left(\Gamma_{eff}\frac{\partial T}{\partial x}\right)+\frac{\partial}{\partial y}\left(\Gamma_{eff}\frac{\partial T}{\partial y}\right) \quad (4)$$

$$\mu_{eff}=\mu+\mu_t, T_0=(T_C+T_h)/2,\ \beta=1/T_0 \quad (5)$$

$$\Gamma_{eff,T}=\frac{\mu}{\Pr}+\frac{\mu_t}{\Pr} \quad (6)$$

The turbulent kinetic energy and the rate of its dissipation for two dimensional buoyancy turbulent flow can be written as follows(**Jones and Luander,1972**):

$$\rho u\frac{\partial k}{\partial x}+\rho v\frac{\partial k}{\partial y}=\frac{\partial}{\partial x}\left(\Gamma_{eff,k}\frac{\partial k}{\partial x}\right)+\frac{\partial}{\partial y}\left(\Gamma_{eff,k}\frac{\partial k}{\partial y}\right)+G-\rho\varepsilon \qquad (7)$$

$$\rho u\frac{\partial \varepsilon}{\partial x}+\rho v\frac{\partial \varepsilon}{\partial y}=\frac{\partial}{\partial x}\left(\Gamma_{eff,\varepsilon}\frac{\partial \varepsilon}{\partial x}\right)+\frac{\partial}{\partial y}\left(\Gamma_{eff,\varepsilon}\frac{\partial \varepsilon}{\partial y}\right)+C_{1\varepsilon}\frac{\varepsilon}{k}G+C_{2\varepsilon}\frac{\varepsilon^2}{k} \qquad (8)$$

where $$G=\nu_t\left[2\left(\frac{\partial u}{\partial x}\right)+2\left(\frac{\partial v}{\partial y}\right)+\left(\frac{\partial u}{\partial y}+\frac{\partial v}{\partial x}\right)\right] \qquad (9)$$

$$\Gamma_{eff,k}=\mu+\frac{\mu_t}{\sigma_k},\ \Gamma_{eff,\varepsilon}=\mu+\frac{\mu_t}{\sigma_\varepsilon} \qquad (10)$$

the eddy dynamic viscosity is obtained by the Prandtl-Kolmogorov hypothesis

$$\nu_t=C_\mu\frac{k^2}{\varepsilon} \qquad (11)$$

the model coefficients are (σ_k ;σ_ϵ ; $C_{1\epsilon}$; $C_{2\epsilon}$; $C\mu$) = (1.0 , 1.3 , 1.44 , 1.92, 0.09) respectively (**Jones and Luander,1972**).

BOUNDARY CONDITIONS

In order to solve the mathematical model, the following boundary conditions are used

At the walls: u = v = 0. and wall function approach (**Versteege and Meer,1995**) is used for the near wall grid points.

For perpendicular walls on the x-axis: at x = 0, T = T_h , at x =L , T = T_c and the parallel walls to the x-axis are insulated.

The local and average Nusselt numbers along the left vertical hot wall can be obtained from the following formulas:

$$Nu=\frac{\partial\Phi}{\partial X}=\frac{\partial T}{\partial x}\frac{L}{T_h-T_C};\quad Nu_{av}=\int_0^1\left(\frac{d\Phi}{dX}\right)dy\approx\frac{1}{N}\sum_{J=1}^{N}\frac{\partial\Phi}{\partial X}$$

The average Nusselt number is a function of Rayleigh and grid points. The number of grid points for $10^8 \le Ra \le 10^{10}$ is 41×41 and for $10^{10} \le Ra \le 10^{16}$ is 84×82 . The increase in Ra needs more grid points and computational time to obtain a converged solutions. The large part of grid points for all the studied Ra are found near the walls in all directions.

NUMERICAL PROCEDURE

Finite volume method is used for the discritisation of the considered governing equations. This gives a system of discritization equations which means that the system of elliptic partial differential equations is transformed into a system of algebraic equations. The solution of these equations is performed by implicit line by line Gause elimination scheme. A computer program is developed to attain the results using the pressure velocity coupling (SIMPLEC algorithm) (**Versteege and Meer,1995**). Due to this strong coupling and non-linearity inherent in these equations, relaxation factors are needed to ensure convergence. The relaxation factors used for velocity components, temperature, pressure and turbulence quantities are 0.4, 0.5, 0.45 and 0.7 respectively. These relaxation factors have been adjusted for each case studied in order to accelerate convergence. Non uniform grid with refinements near the walls is used. The computational grids are staggered for the scalar variables and not staggered for the scalar one. The accuracy of the considered code is validated by comparing the present results with published results as shown in the table 1 . The linear least square regression method is used for the correlation between Ra and Nu_{av} for the present results found in the table 1. This relation takes the form $Nu_{av} = 0.25Ra^{0.40}$

Table1. Comparison of the present results with the published results of (**Marakato,1984**) for Pr=0.71 and $\theta = 0^{\circ}$.

Ra	Nu_{av} (present results)	Nu_{av} (published results)
10^6	8.748	8.754

10^8	32.1	32.04
10^{10}	156.85	156.8
10^{12}	8 40.8	840.1
10^{14}	3627	3624
10^{16}	11229.9	11226

RESULTS AND DISCUSSION

The computed results are presented as follows for different Rayleigh numbers and angles of inclination.

Fig.**2**. demonstrates the stream function for different values of Ra and $\theta = 0^\circ$. It can be seen that at Ra = 10^8, there is two elongated vortices near the enclosure walls. When Ra increased to 10^{10}, the two vortices are stretched to one vorticity in the central part of the enclosure. However there is small vortices arises in the bottom right corner. As Ra =10^{12}, there is small secondary vortices found in the upper part of the enclosure besides the central vorticity. At Ra =10^{14} and Ra =10^{16} the secondary vortices are distributed near the walls. The increasing of Ra due to the increment in H leads to increase the buoyancy which leads to increase the vertical and horizontal velocities consequently effect on the vorticity distribution. The effect of angle of inclination on stream function distribution for Ra = 10^8 is depicted in **Fig**.**3**. As the Figure shows, when $\theta = 30^\circ$, the stretching vortices are elongated in the direction of inclination and the size of the occupied region by these vortices is less compared with the case of $\theta = 0^\circ$. When $\theta = 60^\circ$, besides to the elongated vortices, there is a small secondary vortices near the enclosure walls. The size of these vortices is larger compared with $\theta = 30^\circ$. At $\theta = 90^\circ$ there is four re-circulating secondary vorticties formed near the vertical walls and bottom surface as a result of increasing the buoyancy force because the hot wall became at the bottom . As the angle increased to $\theta = 120^\circ$, there is elongated vortices and two secondary vortices near the walls. The occupied zone by the elongated vortices is larger. For $\theta = 150^\circ$, the distribution is nearly similar to the case of $\theta = 30^\circ$. However the boundary layer is thicker. This is demonstrated at **Fig**.**6** and **Fig**.**8**.

For $\theta = 180^\circ$ there is two secondary vortices and the size of these vortices is larger compared with the case of $\theta = 0^\circ$. The temperature distribution for different Rayleigh numbers and $\theta = 0^\circ$ is shown in **Fig**.**4**. It is evident that the heat is transferred from the hot wall to the cold wall through a working fluid (air) by convection. This assessed when one observe that the isotherm lines are not perpendicular. Also it can be seen that the thermal boundary layer thickness as shown in b,c,d and e. is decreased with the increase of Ra and as a consequence of this the rate of heat transfer is faster with increasing the Rayleigh number. The temperature distribution for different angles of inclination and Ra=10^8 is shown in **Fig**.**5**. It can be seen that at $\theta = 30^\circ$, the isotherm lines are inclined with direction of the enclosure tilted angle and the rate of heat transfer is less compared with case of $\theta = 0^\circ$. The isotherm lines be thicker at the lower part of the hot wall and upper part of the cold one and this leads to the rate of heat transfer to be larger. This confirmed through **Fig**.**6**. which demonstrates the variation of the average Nusselt number with angles of inclination. As **Fig**.**5**. shows, the rate of heat transfer is continous to decrease from $\theta = 60^\circ$ to $\theta = 90^\circ$. At $\theta = 120^\circ$ to $\theta = 180^\circ$, the rate of heat transfer is noticeably increased and this confirmed at **Fig**.**6**.. Also it can be seen from **Fig**.**6** that the average Nusselt number is increased with the increase of Ra for all angles of inclination because when Ra is increased, the buoyancy induced flow is increased and that leads to increase the rate of heat transfer. The local nusselt number variation along the hot wall for different Ra and $\theta = 0^\circ$ is depicted in **Fig**.**7**. It can be seen that the the lower corner of the hot wall indicated the high value of Nu and hence the high rate of heat transfer. When the enclosure is tilted with the considered angles of inclination($0 \le \theta \le 90 \deg.$), **Fig**.**8**., the local Nusselt number values is decreased. It is evident that for $\theta = 30^\circ$ to $\theta = 90^\circ$, the lower corner(y/H=0) of the hot wall disclosed the high values of Nu while at $\theta = 120^\circ$ to $\theta = 180^\circ$, this position is shifted to y/H=0.95 as a

result of change of the location of hot and cold walls and hence changing the strength of buoyancy force.

CONCLUSIONS

In the present paper, the turbulent 2D natural convection inside inclined square enclosure has been successfully predicted. From the computed results, the following conclusions can be obtained.

- The rate of heat transfer is increased with the increase of Ra and decreased with the increase of angle of inclination($0 \le \theta \le 90 \deg.$) and converse verse at($90 \le \theta \le 180 \deg.$) .
- The local Nusselt number values along the hot tilted wall is higher at the bottom section of the wall, while for the tilted cold wall at the top section.
- The thermal boundary layer thickness is decreased with the increase of Ra
- The resulted vortices are stretched to the middle of the enclosure with the increase of Ra.

REFERENCES

-Ampofo, F., Karayiannis, T.G., " Experimental benchmark data for turbulent natural convection in an air filled square cavity", Int. J. Heat Mass Transfer, vol.46, 2003.

-Corcione, M., " Effect of thermal boundary conditions at side walls upon natural convection in rectangular enclosures heated from below and cooled from a bove", Int. J. Thermal Sci. vol.42, 2003.

-El shirbiny, S.M., Hollands, G.D., Raithby, " Nusselt number distribution in a vertical and inclined air layers", J. heat Transfer, 1983.

-Elshirbiny, S.M., Hollands, G.D., " Heat transfer by natural convection across vertical and inclined air layers", J. Heat Transfer 104, 1982.

-Ganzarolli, M.M, Milane Z, L.F., " Natural convection in rectangular enclosures heated from below and symmetrically cooled from the sides", Int. J. Heat and Mass Transfer, 1995.

-Hart,E.J., "Stability of the flow in a differentially heated inclined box", J. Fluid Mech.,1971.

-Jones, W.P., Lunder, B.E., The prediction of laminarization with a two equation model of turbulence", J. Heat and Mass transfer, 1972

-Kuyper, R.A, Van Der Meer, C.J., Henkes, R.A.," Numerical study of laminar and turbulent natural convection in an inclined square cavity, Int.J. Heat mass Transfer,36,1993.

-Lankhorst, A.M., Henkes, Hoogendoorn, C.J.,'' Natural convection in cavities at high Rayleigh numbers", second UK national conference on heat transfer, university of Strathclycle, Glasgow, 1991

-Markatos, N.C., Pericleous, K.A., " Laminar and turbulent natural convection in an enclosed cavity", Int. J. Heat mass transfer, 1984.

-Osttrach, S., " Natural convection in enclosure", J. heat Transfer Trans., ASME, 1988.

Vahl Davis, G.De., " Natural convection in a square cavity, a comparison exercises", Int. J. Numer. Methods Fluids, 1983.

-Versteege, H. and Meer, W." An introduction of computational fluid dynamics", Hemisophere Publishing Corporation, United State of Americs, 1995.

-Zhong, Z.Y., Yang, K.T., " Variable property natural in tilted cavities with thermal radiation", Numerical Methods in Heat Transfer, vol.3, 1985.

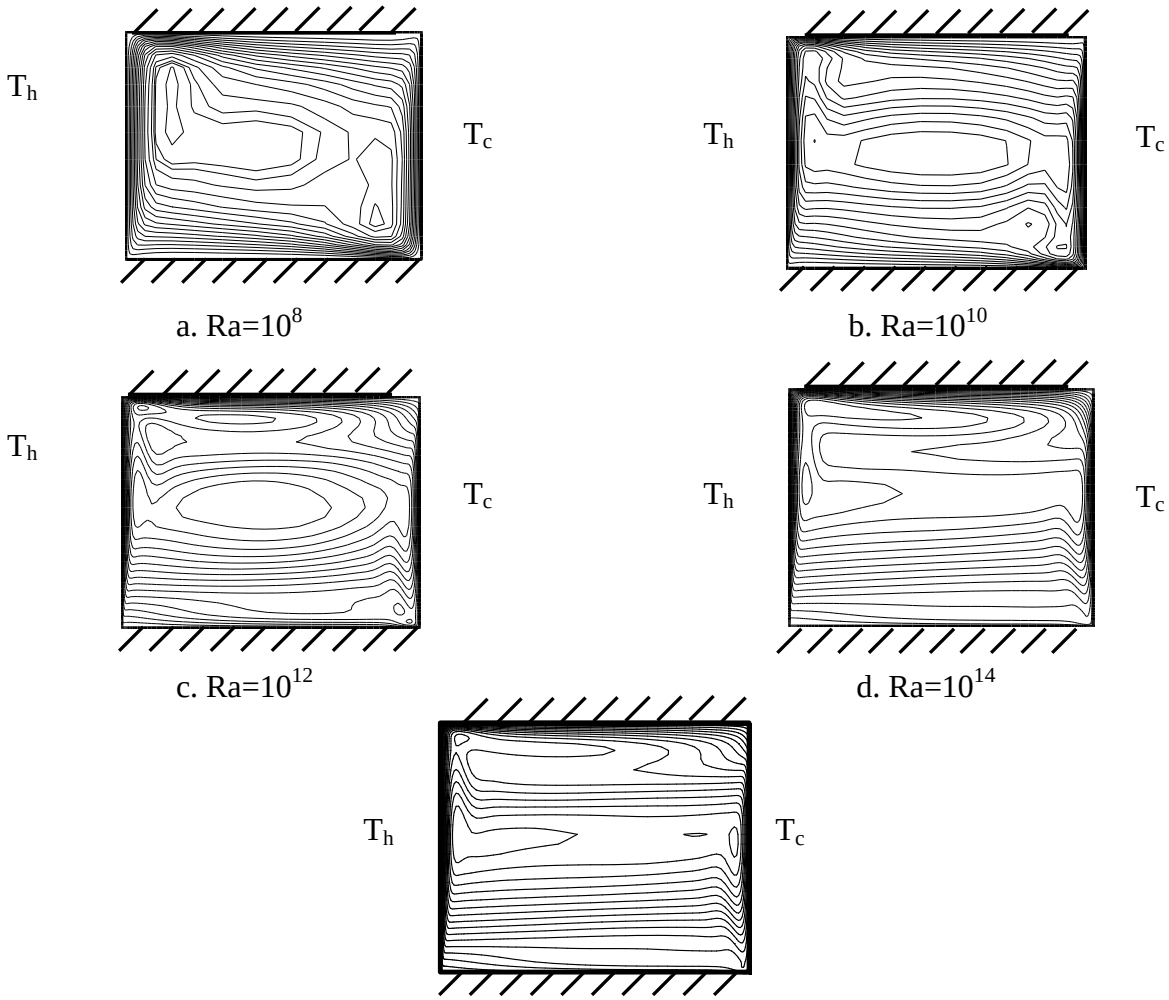

Fig.2. stream function distribution at different Ra and. $\theta = 0^\circ$

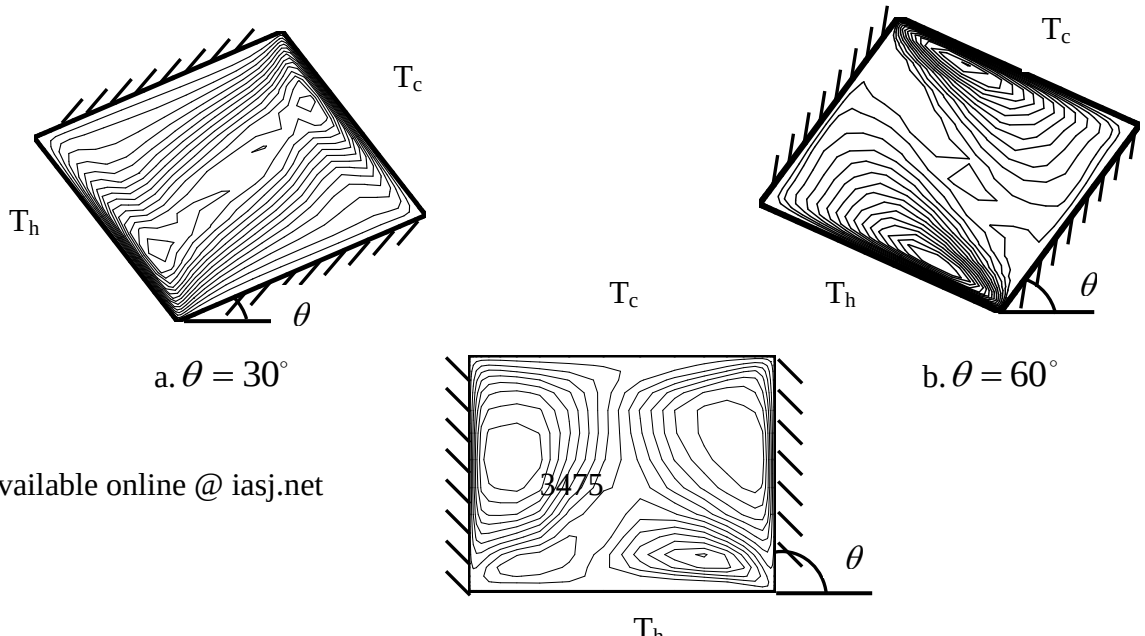

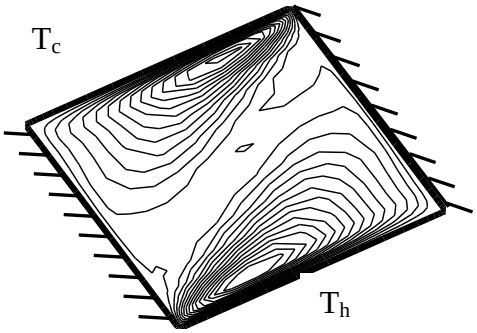

d. $\theta = 120^{\circ}$

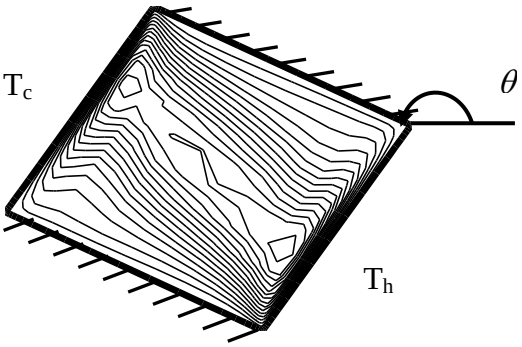

e. $\theta = 150^{\circ}$

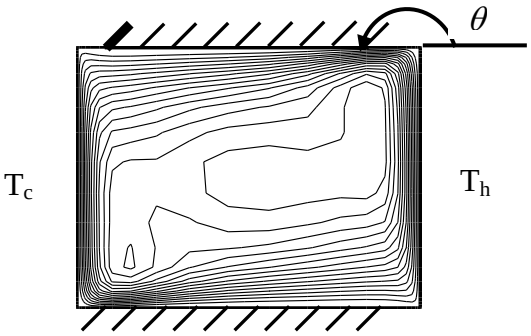

f. $\theta = 180^{\circ}$

Fig.3. stream function distribution at different angles of inclination and Ra=10^8

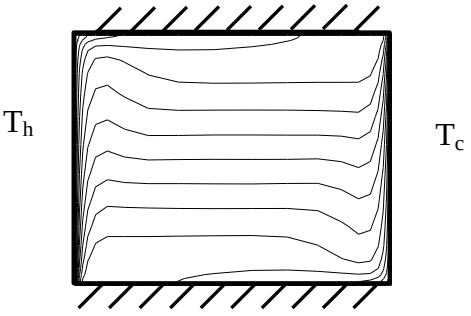

a. Ra=10^8

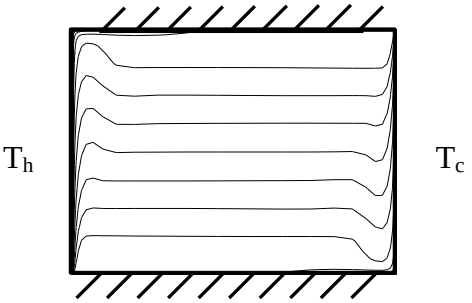

b. Ra=10^{10}

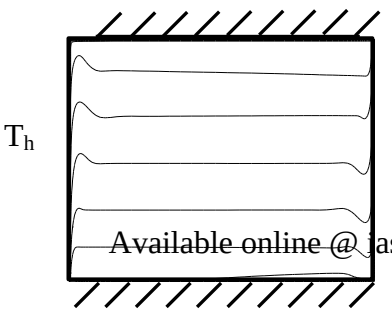

c. Ra=10^{12}

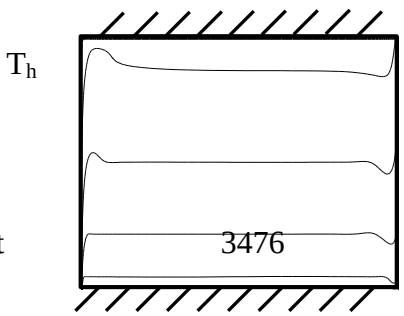

d. Ra=10^{14}

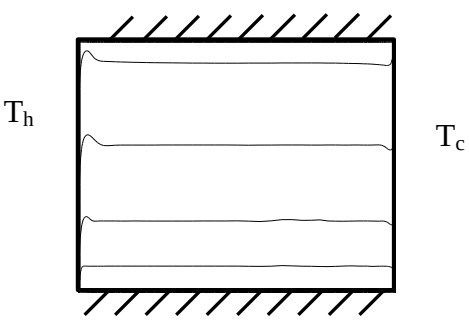

e. Ra=10^{16}

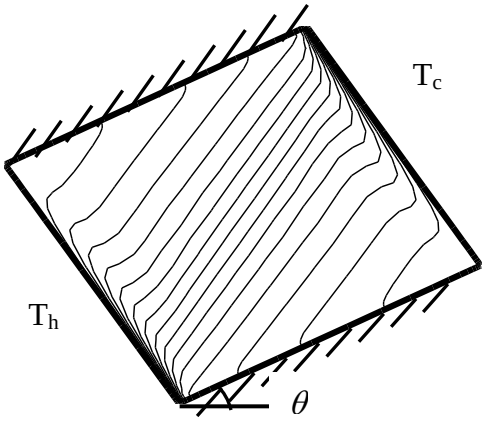

a. $\theta = 30^\circ$

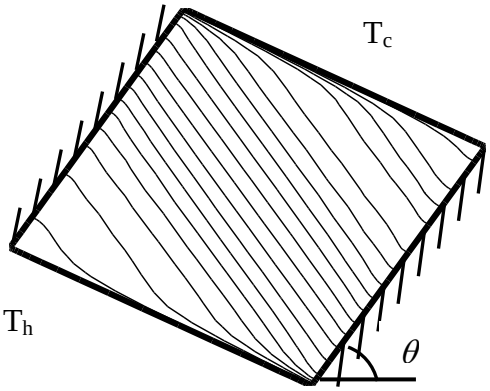

b. $\theta = 60^\circ$

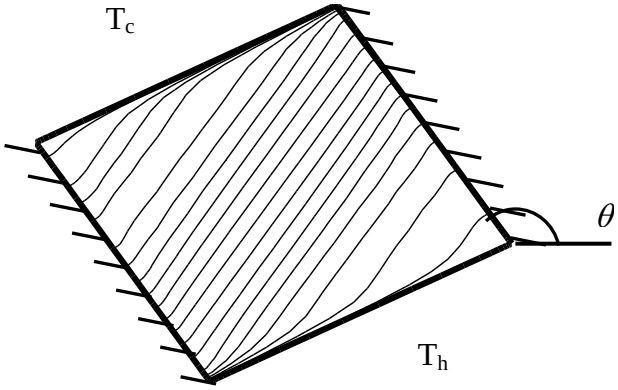

c. $\theta = 120^\circ$

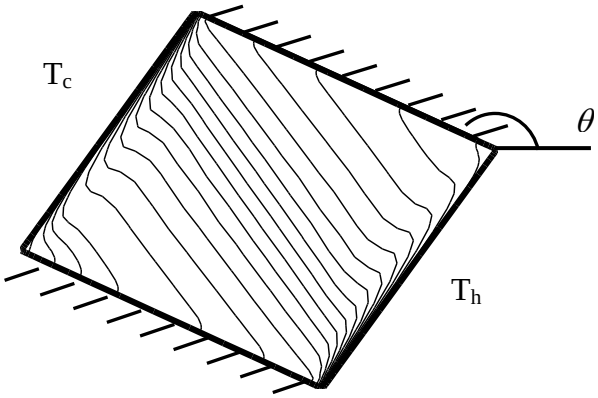

d. $\theta = 150^\circ$

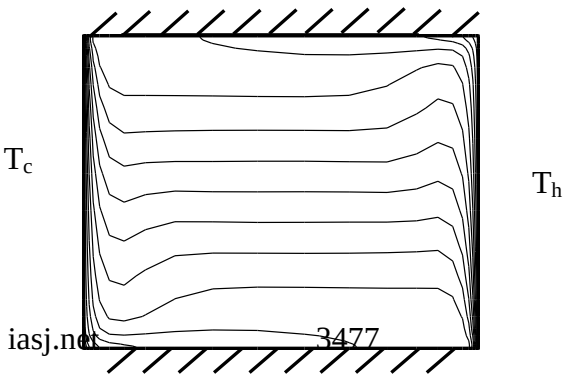

e. $\theta = 180^\circ$

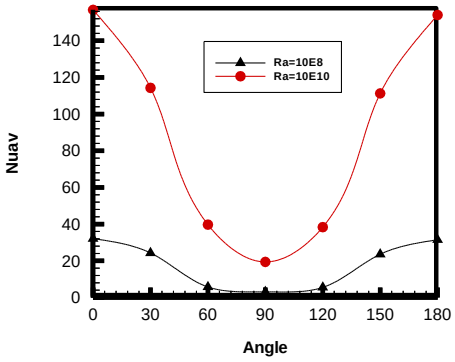

a

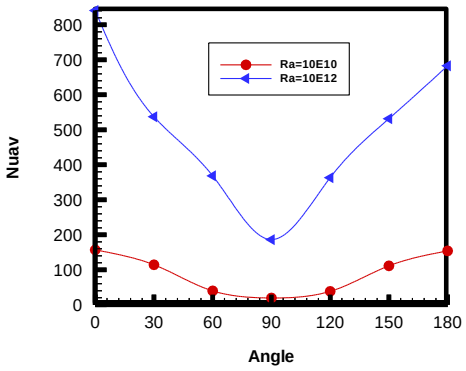

b

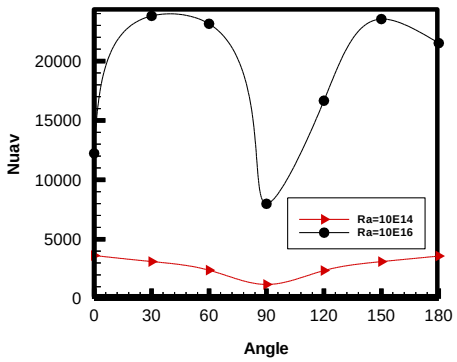

c

Fig.6. variation of average Nusselt number with angles of inclination at different Rayleigh numbers

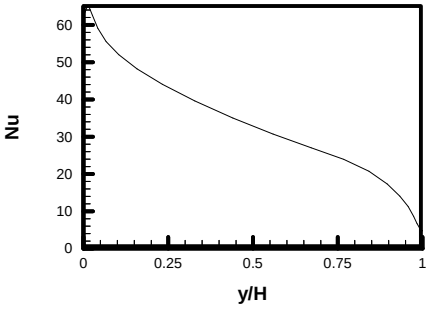

a.

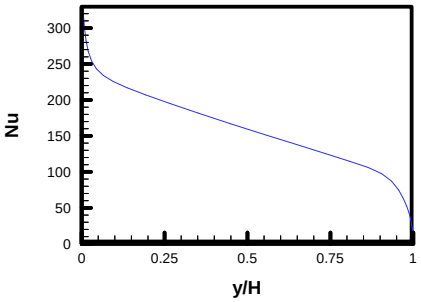

b.

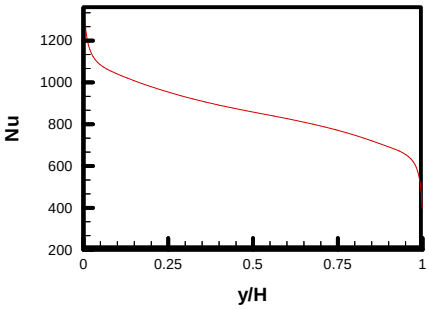

c.

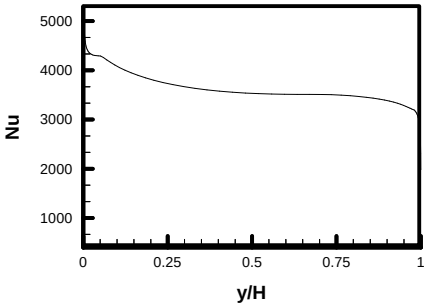

d.

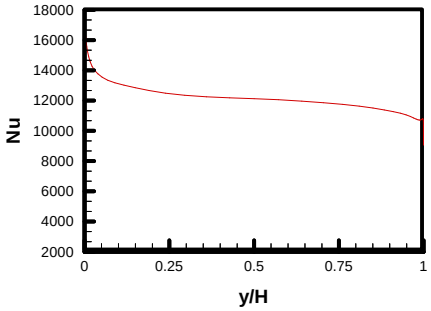

e.

Fig.7. Local Nusselt number variation at the hot wall (x=0) for different Ra; a. Ra=10^8; b. Ra=10^{10}; c. Ra=10^{12}; d. Ra=10^{14} e. Ra=10^{16}

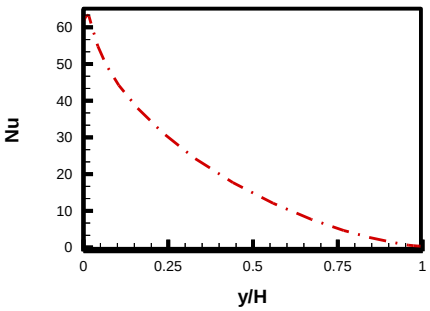

a. $\theta = 30^{\circ}$

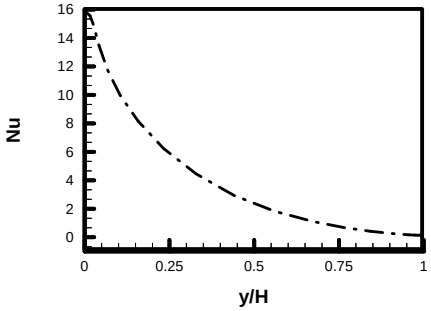

b. $\theta = 60^{\circ}$

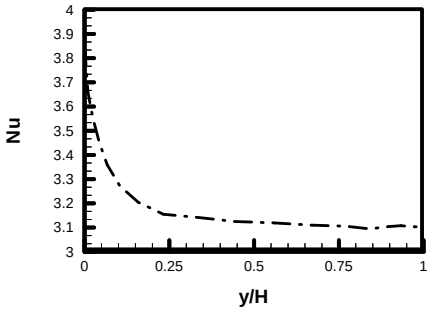

c. $\theta = 90^{\circ}$

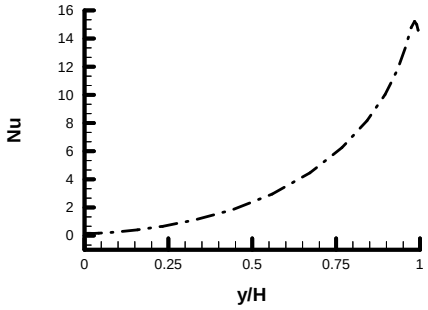

d. $\theta = 120^{\circ}$

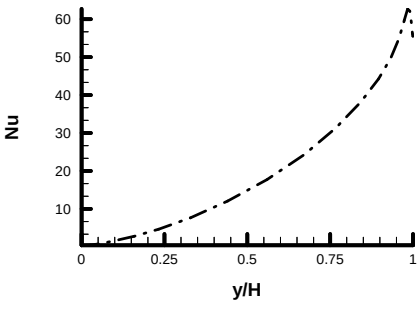

e. $\theta = 150^{\circ}$

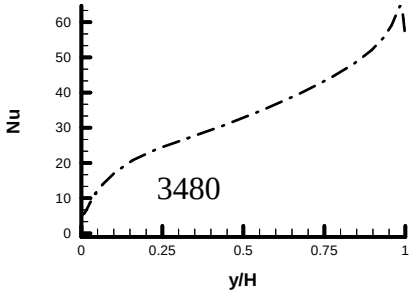

NOMENCLATURE

C_u, $C_{1\varepsilon}$, $C_{2\varepsilon}$	turbulence constants, -
G	generation term by shear, Kg/m.sec^3
H	height of the enclosure, m
k	turbulent kinetic energy, m^2/s^2
Nu	local Nusselt number, -
Nu_{av}	average Nusselt number, -
P	pressure, N/m^2
Pr	Prandtl number, -
Ra	Rayleigh number $\left(\frac{g\beta H^3(T_h - T_c}{\alpha\mu}\right)$, -
T_C	cold wall temperature, Ċ
T_h	hot wall temperature, Ċ
x, y	Cartesian coordinates, m
X	dimensionless Cartesian coordinate $\left(\frac{x}{H}\right)$,-

Greak symbols:

ϵ	turbulance dissipation rate, m^2/s^3
μ	dynamic viscosity, N.s/m^2
μ_t	turbulent viscosity, N.s/m^2
v_t	eddy dynamic viscosity, m^2/s
μ_{eff}	effective turbulent viscosity, N.s/m^2
Γ_{eff}	effective exchange coefficient, kg/m.s

Φ dimensionless temperature $\left(\frac{T-T_c}{T_h-T_c}\right)$, -

σ_k ;σ_ϵ turbulent schmidt numbers, -

α thermal diffusivity of fluid, m^2/s